

## Microtremor-Based Mitigation Pathways and Disaster Post Placement in the Merapi Geotourism Area, Yogyakarta

Kesya Lutfiany Fatihah<sup>1\*</sup>, Maria Diyah Ayu Wulandari<sup>2</sup>, Anwar Said Pintrandhita<sup>3</sup>, Ryan Surya Dharma Tarigan<sup>4</sup>

1. UPN Veteran Yogyakarta, Indonesia
2. UPN Veteran Yogyakarta, Indonesia
3. UPN Veteran Yogyakarta, Indonesia
4. UPN Veteran Yogyakarta, Indonesia

### ARTICLE INFO:

**Submitted:** December 16<sup>th</sup>, 2024

**Revised:** January 8<sup>th</sup>, 2025

**Accepted:** January 8<sup>th</sup>, 2025

**Section:** Tourism

### Corresponding Author:

Kesya Lutfiany Fatihah

### Corresponding Author Email:

115210051@student.upnyk.ac.id

**ABSTRACT:** Cangkringan District, located on the slopes of Mount Merapi, is highly susceptible to volcanic and seismic activity, posing risks to its residents and the thriving geotourism sector. This study aims to determine optimal mitigation pathways and disaster post placements using geophysical methods, specifically the HVSR microtremor method and GGMPPlus satellite gravity data. The research analyzed seismic vulnerability, ground acceleration, and shear wave velocity ( $V_{s30}$ ), combined with gravity anomaly data, to identify high-risk areas and safe zones. The results produced a detailed mitigation map, guiding the placement of two disaster posts and evacuation routes based on soil vulnerability, topography, and rock density. These findings contribute to disaster risk reduction efforts and sustainable geotourism development by enhancing evacuation efficiency and safety for residents and tourists. This integrated approach offers a model for disaster-prone regions, balancing economic growth with safety and resilience against geological hazards.

**Keyword:** GGMPPlus, microtremor, mitigation, Mount Merapi

## INTRODUCTION

Mount Merapi, one of the most active volcanoes in Indonesia, poses significant risks due to frequent volcanic and tectonic activities. The surrounding regions, particularly Cangkringan District in Sleman Regency, Yogyakarta, are highly vulnerable to disasters triggered by volcanic eruptions and earthquakes. This region, known for its unique blend of geotourism attractions, combines natural and artificial tourism features that attract thousands of visitors annually. Despite the area's tourism potential, insufficient disaster mitigation measures have been implemented, leaving residents and tourists exposed to significant risks. Addressing these challenges is crucial for ensuring the safety and sustainability of tourism in this high-risk area.

Geotourism, as a concept, emphasizes sustainable tourism development in areas with unique geological features, combining education, conservation, and economic benefits (Dowling, 2011). However, the safety of tourists and residents must remain a primary concern, particularly in disaster-prone regions.



Effective disaster mitigation strategies rely on comprehensive geophysical analyses to identify high-risk zones and safe evacuation routes. Recent advancements in geophysical methods, including the HVSr microtremor and gravity anomaly techniques, offer precise tools for assessing subsurface vulnerability (Alonso-Pandavenes et al., 2023; Nakamura, 1999). Utilizing these methods allows for a deeper understanding of geological hazards and supports informed decision-making for disaster management.

In regions like Cangkringan, where volcanic and seismic hazards overlap with high tourism activity, disaster risk reduction must align with sustainable development goals. The integration of geophysical data into disaster preparedness frameworks can mitigate risks and enhance community resilience. Previous studies have demonstrated the effectiveness of microtremor methods in mapping seismic susceptibility and identifying areas prone to liquefaction and landslides (Beroya et al., 2009; Diaz-Segura et al., 2024; Liu et al., 2023; Putriani et al., 2023). Such analyses, when combined with gravity data, provide a robust foundation for designing evacuation routes and disaster mitigation posts, ensuring both residents' and tourists' safety.

This study focuses on identifying safe zones and optimal locations for disaster posts in Cangkringan District by integrating microtremor data with satellite-based gravity analysis. By creating seismic vulnerability maps and analyzing ground shear strain, the study determines areas with the lowest geological risks. These findings contribute to disaster management by improving evacuation infrastructure and increasing public awareness of disaster preparedness. Moreover, the integration of these methodologies aligns with global disaster risk reduction frameworks, such as the Sendai Framework for Disaster Risk Reduction (Bailey, 2022; Pant, 2023; Zewde, 2023), which emphasizes the importance of understanding risks to enhance resilience.

Through the development of mitigation maps and the strategic placement of disaster posts, this research aims to create a safer geotourism framework for the Merapi slope. The findings not only contribute to local disaster preparedness but also offer valuable insights for other geologically vulnerable areas worldwide. By combining advanced geophysical techniques and practical disaster mitigation strategies, this study addresses the pressing need for safety and resilience in high-risk tourism destinations while promoting sustainable development.

## LITERATURE REVIEWS

### Geological of Merapi Mountain

Mount Merapi, a prominent active volcano in Indonesia, exhibits a complex geomorphological structure that can be divided into four distinct landforms, each shaped by its volcanic origins (Surono et al., 2012; Thouret et al., 2000). The first landform, the Lava Dome (V1), occupies approximately 5% of Mount Merapi's area and lies at an altitude of 2885-2900 meters above sea level (masl). This dome, formed by volcanic activity, continues to grow and is susceptible to destruction during eruptions. The second landform, the Lava Flow Slope (V2), comprises 55% of the volcano's area, with altitudes ranging from 2250 to 2860 masl. This slope results from the accumulation of lava that flows down during eruptions.

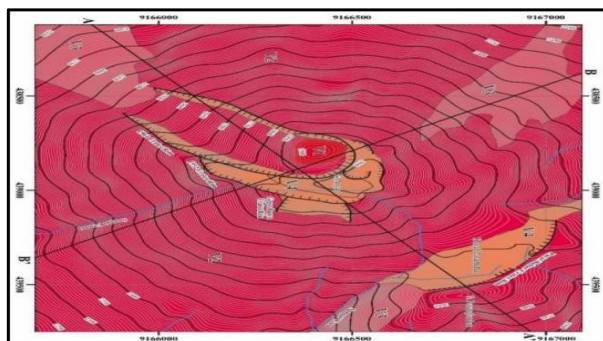


**Figure 1.** Landforms of Mount Merapi and Surroundings  
Source: Yudiantoro et al. (2023)

The third landform, the Pyroclastic Flow Slope (V3), covers 25% of Mount Merapi and is situated near the northwest-southwest slopes of the summit, particularly around the Pasarbubrah Crater. At altitudes between 2250 and 2750 masl, this area is shaped by pyroclastic flows that travel through crater openings into river valleys and wild channels. Finally, the Crater (V4) accounts for 15% of the volcano's area and is located at the summit. The crater's expanse follows the openings towards the southwest slope, including the Pasar Bubrah Crater. These geomorphic divisions reflect the dynamic volcanic activity shaping Mount Merapi's landscape over time.

Stratigraphically, Mount Merapi's volcanic structure comprises rock units formed in two distinct phases, Old Merapi and Young Merapi, each with unique characteristics (Yudiantoro et al., 2023). The Old Merapi phase features andesite lava flows, primarily located at the summit and its surrounding areas. This phase represents the initial volcanic activity that laid the foundation of the mountain. In contrast, the Young Merapi phase is associated with more recent volcanic activities, including new crater formations at the summit and pyroclastic flows extending southwest. Key features include lava flows from both historical and post-historical eruptions, along with deposits in the Pasar Bubrah crater and northeast of the peak. These layers comprise Merapi andesite lava flows 3 and 4, young pyroclastic deposits, and additional andesite formations.

Together, Mount Merapi's geomorphic and stratigraphic features provide critical insights into its dynamic volcanic processes, shaping both its physical structure and the associated risks for surrounding communities and geotourism activities.

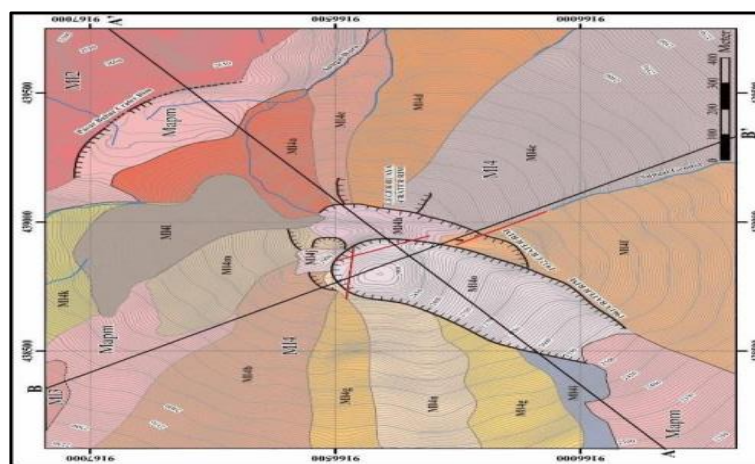


**Figure 2.** Geological Map of Mount Merapi's Summit and Surroundings  
Source: Yudiantoro et al. (2023)

In stratigraphic terms, the volcano stratigraphic setting and rock units at the summit of Mount Merapi and its surroundings are from the oldest to the youngest in age (Yudiantoro et al., 2023): (a) Old Merapi: Located on the summit of Mount Merapi and its surroundings with rock units in the form of Merapi 2 andesite lava flows. (b) Young Merapi: Located in the new crater of the peak of Mount Merapi, crater openings to the southwest, former lava flows before and after the historical period and new pyroclastic flows, including the Pasar Bubrah crater in the northeast of the peak with rock units of Merapi andesite lava flows 3, young pyroclastic deposits and Merapi lava flows, and deposits of Merapi andesite lava flows 4.

### Microtremor Method

The microtremor method is a non-invasive geophysical technique designed to monitor and analyze low-frequency ground vibrations, often referred to as microseisms. These vibrations are generated by natural phenomena such as earthquakes, tectonic activity, volcanic processes, and even human-induced factors like industrial operations. The method focuses on measuring the amplitude and frequency of these ground

vibrations, typically within a frequency range of 0.1–1 Hz, using highly sensitive seismometers capable of detecting even the smallest ground movements (Hou et al., 2021; Sollberger et al., 2020).

One of the primary advantages of the microtremor method is its ability to provide rapid and cost-effective measurements while yielding detailed insights into subsurface soil properties. Unlike other geophysical techniques, it requires minimal field intervention, making it an ideal choice for large-scale or preliminary assessments of geological vulnerability. Its affordability and non-invasive nature further enhance its applicability, particularly in urban and sensitive areas where disruptive methods are impractical.

The method has gained significant utility in geotechnical modeling and seismic hazard assessment. By analyzing microtremor data, engineers can identify soil amplification factors, sediment thickness, and seismic vulnerability indices in specific locations. These insights are crucial for designing structures with enhanced earthquake resistance, ensuring the safety and durability of infrastructure in high-risk areas. For instance, the method allows engineers to determine areas prone to ground motion amplification and liquefaction, enabling targeted interventions to mitigate risks.

Additionally, the microtremor method supports urban planning and disaster mitigation strategies by generating detailed micro zonation maps. These maps are invaluable for identifying high-risk zones, guiding the placement of disaster posts, and planning evacuation routes in areas susceptible to earthquakes and other seismic activities. Its application extends to assessing the structural integrity of existing buildings and infrastructure, aiding in retrofitting strategies to enhance resilience.

Overall, the microtremor method is a versatile and efficient tool that bridges the gap between theoretical geophysical studies and practical engineering applications. By providing a deeper understanding of subsurface conditions, it contributes significantly to disaster risk reduction, infrastructure resilience, and sustainable urban development in seismically active regions.

### **Horizontal to Vertical Spectral Ratio**

The Horizontal to Vertical Spectral Ratio (HVSR) method is a widely utilized technique in geophysics to analyze soil dynamics and subsurface characteristics. It is based on microtremor waves, which are natural seismic vibrations caused by a combination of tectonic activity, volcanic eruptions, and human-induced activities such as traffic or construction (Neukirch et al., 2021). These microtremor waves are omnipresent and provide valuable information about the dynamic properties of the soil and subsurface layers.

The HVSR method operates by comparing the Fourier spectra of the horizontal and vertical components of microtremor waves. The Fourier spectrum represents the distribution of wave energy across different frequencies, allowing researchers to identify dominant frequencies and amplitudes associated with specific subsurface conditions. This ratio provides a simple yet effective way to estimate soil response to seismic events and determine key parameters such as soil resonance frequencies, sediment thickness, and subsurface lithology.

One of the significant advantages of the HVSR method is its non-invasive nature, making it suitable for urban and environmentally sensitive areas. It is particularly effective in identifying resonant frequencies of soil layers, which are critical for understanding site-specific seismic amplification. High HVSR values often indicate soft or loose soil layers with low density, which are more prone to seismic amplification and liquefaction during earthquakes. Conversely, low HVSR values suggest dense or hard rock formations with higher resistance to seismic waves.

The HVSR curve, derived from the spectral analysis, is essential for interpreting subsurface conditions. Peaks in the HVSR curve correspond to the dominant frequency of the soil, which is controlled by factors such as subsurface velocity, sediment thickness, and the contrast between soil layers. For example, regions with thick sediment deposits typically exhibit lower dominant frequencies, while areas with thin or hard rock layers show higher dominant frequencies.

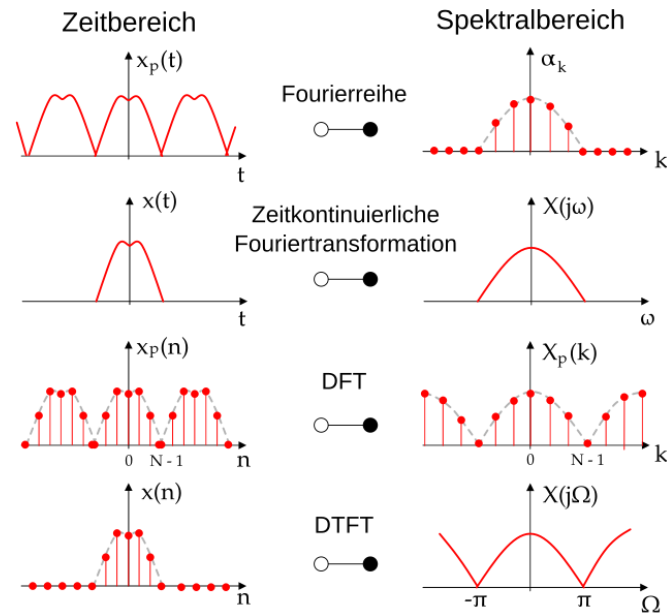


**Figure 3.** Spektrum Fourier  
Source: [Brigola \(2025\)](#)

In Figure 3, the Fourier spectrum representation provides a visual understanding of how the HVSR method works. The horizontal axis depicts frequency (Hz), while the vertical axis shows amplitude or spectral ratio. The horizontal and vertical components of the microtremor waves are plotted, and their ratio is calculated at each frequency point. Peaks in the HVSR curve indicate soil resonance, providing insights into the soil's dynamic response to seismic waves.

This method is widely applied in earthquake risk assessment, geotechnical engineering, and urban planning. By identifying zones with high seismic amplification potential, the HVSR method aids in the design of earthquake-resistant structures and the development of disaster mitigation strategies. Moreover, its ability to map subsurface features makes it a crucial tool for understanding local geology and improving infrastructure resilience in seismically active regions.

### Gravity Method

The gravity method is a geophysical technique widely employed in subsurface exploration, particularly for identifying structural anomalies and regional geological features. This method leverages variations in gravitational acceleration caused by differences in rock density and elevation within the subsurface. By measuring gravity values across a study area, geophysicists can infer the distribution and composition of underlying geological structures ([Mishra, 2024](#)). This technique is especially valuable for mapping large-scale features such as faults, basins, and volcanic formations, making it indispensable in resource exploration, seismic studies, and disaster mitigation planning.

At the core of the gravity method lies the concept of gravity anomalies, which represent deviations from the Earth's standard gravitational field. These anomalies are influenced by variations in subsurface rock density, with denser materials producing higher gravity values and less dense materials producing lower values. To accurately analyze these deviations, the gravity method applies corrections to account for factors such as topography, instrument drift, tidal effects, and variations in Earth's gravitational field due to altitude differences. This comprehensive correction process ensures that the measured anomalies reflect true subsurface characteristics.

A critical aspect of gravity anomaly analysis is the Complete Bouguer Anomaly (CBA), which refines raw gravity measurements to account for various corrections. The CBA calculation incorporates adjustments for instrumental errors, normal gravity correction for the Earth's curvature, elevation-related

effects, and terrain correction to address the influence of nearby topographic features. The formula for the Complete Bouguer Anomaly is expressed as:

$$CBA = A_{gobs} - g_n + 0.3086h - 0.04192ph + TC$$

Where:

- CBA : complete Bouguer anomaly
- $A_{gobs}$  : gravity measurement result
- $g_n$  : gravity value in the spheroid plane
- $h$  : altitude of the measurement station location
- $p$  : average density
- TC : terrain correction

## METHODS

The study was conducted in the Cangkringan District, Sleman Regency, Yogyakarta Special Region, which is highly susceptible to seismic and volcanic hazards due to its proximity to Mount Merapi. To analyze the subsurface conditions and seismic risks in this area, the research employed two complementary geophysical methods: the micro seismic method and the gravity method. These techniques were combined with Landsat satellite imagery to enhance spatial accuracy and provide a comprehensive understanding of the region's geological characteristics. The data collection and analysis were carried out over a 1.3 x 1 km study area, with 17 measurement points distributed systematically, as illustrated in Figure 4: Acquisition Design of Microseismical.

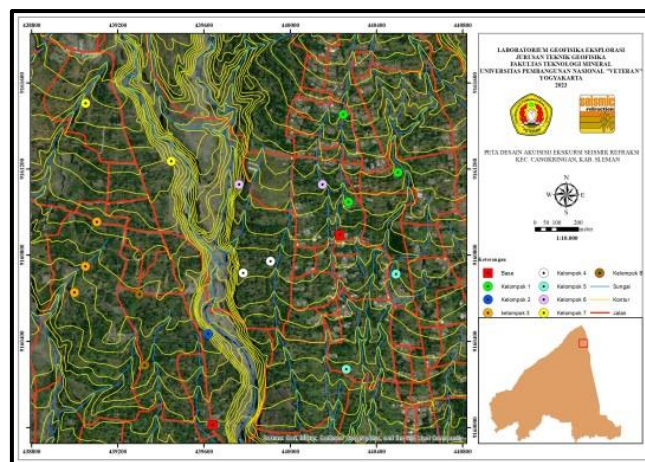


**Figure 4.** Acquisition Design of Microseismical  
Source: Data processing, 2024

The micro seismic method utilized microtremor data, which involves capturing low-frequency ground vibrations. Data acquisition was performed using three-component sensors (X, Y, Z) at each of the 17 designated points within the study area. These sensors recorded microtremor waveforms, which were subsequently processed to derive key seismic parameters. The microtremor measurements focused on frequencies below 3 Hz to capture subsurface dynamics accurately.

After acquiring the raw data, several processing steps were conducted to ensure accuracy and reliability. The data underwent filtering to remove noise and artifacts, followed by quality control checks to validate the results. The processed data were used to generate the HVSr curve, which represents the Horizontal to Vertical Spectral Ratio. This curve provided information on dominant frequency and amplification values, essential for identifying areas prone to seismic amplification.

The next step involved calculating seismic susceptibility ( $K_g$ ), which indicates the vulnerability of soil and subsurface layers to seismic activity. This calculation used the dominant frequency and amplification data derived from the HVSR curve. Additionally, the data were inverted using the Dinver software to estimate  $V_{s30}$  values, which represent the average shear wave velocity at a depth of 30 meters.  $V_{s30}$  is a critical parameter for assessing soil stiffness and seismic hazard.

To estimate the Peak Ground Acceleration (PGA), which measures the maximum ground shaking intensity during an earthquake, relevant earthquake data were incorporated into the analysis. The PGA values were then used to calculate Ground Shear Strain (GSS), a parameter that combines seismic susceptibility and ground acceleration to assess potential building damage and soil deformation. These parameters collectively allowed the creation of a micro zonation map, which highlights zones with varying seismic risks.

The gravity method complemented the micro seismic analysis by providing insights into subsurface density variations. Data from the GGMPlus high-resolution satellite gravity database were utilized to extract the Free Air Anomaly (FAA) values for the study area. These values were further processed to produce the Complete Bouguer Anomaly (CBA) map. The CBA accounts for corrections such as topography, altitude, and density variations, offering a detailed representation of subsurface geological structures.

The gravity method involved analyzing differences in gravitational acceleration caused by variations in rock density and topography. The extracted gravity anomalies helped identify high- and low-density zones, such as sedimentary layers, volcanic deposits, and igneous formations. By integrating the CBA map with the micro seismic data, a comprehensive geological profile of the study area was developed.

The final step of the analysis combined the results of the micro seismic and gravity methods to create a mitigation map for the study area. The micro zonation map, derived from micro seismic parameters, was overlaid with gravity data to identify safe zones and high-risk areas. Specific parameters, such as  $V_{s30}$ , seismic susceptibility, and GSS, were used to pinpoint optimal locations for disaster mitigation posts and evacuation routes.

The mitigation map highlights areas with low seismic vulnerability and dense subsurface materials, making them suitable for disaster response infrastructure. Conversely, high-risk zones, characterized by soft soils and high seismic susceptibility, were marked as areas to avoid during evacuation. This integrated approach ensures that the mitigation strategies are both scientifically robust and practically applicable.

By combining advanced micro seismic and gravity techniques, this study provides a detailed understanding of the geological risks in Cangkringan District. The development of the mitigation map serves as a critical tool for disaster preparedness and risk reduction, benefiting both local residents and geotourism activities in the region. These methods can be adapted and applied to other disaster-prone areas, making them invaluable for sustainable development and resilience planning.

## RESULTS AND DISCUSSION

### Amplification

Amplification refers to the propagation of seismic waves caused by variations in subsurface material properties, particularly differences in rock density and sediment thickness. These variations lead to the amplification of seismic waves, increasing the intensity of ground shaking during an earthquake. Amplification is a crucial parameter for assessing seismic hazards, as areas with higher amplification values are more likely to experience severe damage during seismic events (Nakamura, 1999).

In this study, amplification values were calculated using the HVSR microtremor method. The results showed amplification values ranging from 0.5 to 7.5 Hz, which were classified into four distinct categories based on Table 1. These categories are low amplification ( $A < 3$ ), medium amplification ( $3 \leq A < 6$ ), high amplification ( $6 \leq A < 9$ ), and very high amplification ( $A \geq 9$ ) (Yulianto & Yuliyanto, 2023). This classification provides a clear understanding of the seismic vulnerability of the study area, helping to identify zones with varying degrees of seismic risk.

**Table 1.** Classification of Amplification Values

Zone	Classification	Amplification Value
1	Low	$A < 3$
2	Medium	$3 \leq A < 6$

3	High	$6 \leq A < 9$
4	Very High	$A \geq 9$

Source: [Yulianto & Yuliyanto \(2023\)](#)

The amplification map of the Cangkringan Sub-District, presented in Figure 5, illustrates the spatial distribution of amplification values across the region. Areas with high amplification values, represented in red, indicate zones with low-density or soft rock. These areas are the most susceptible to seismic wave amplification and are considered high-risk zones for structural damage during an earthquake. Medium amplification values, represented in yellow and green, correspond to regions with moderately dense rock and a lower susceptibility to seismic amplification compared to high-risk zones. Conversely, low amplification values, represented in blue, are associated with dense rock formations. These areas are less prone to seismic amplification and are considered relatively safer during seismic events.

The results from this study provide critical insights into the spatial variability of seismic risks. High-amplification zones, located in areas with soft rock or thick sediment deposits, should be prioritized for disaster risk reduction measures. These areas are unsuitable for critical infrastructure and residential development due to their heightened susceptibility to damage during earthquakes. In contrast, low-amplification zones with dense rock formations are more suitable for the placement of evacuation routes and disaster mitigation posts, as they are less vulnerable to seismic amplification.

The amplification map, along with other seismic parameters such as seismic susceptibility (Kg), Peak Ground Acceleration (PGA), and Vs30 values, forms the foundation for a comprehensive seismic risk assessment of the study area. By integrating these datasets, the study identified optimal locations for disaster mitigation posts and safe evacuation routes. This approach ensures that disaster preparedness strategies are scientifically informed and effectively mitigate risks for both residents and tourists.

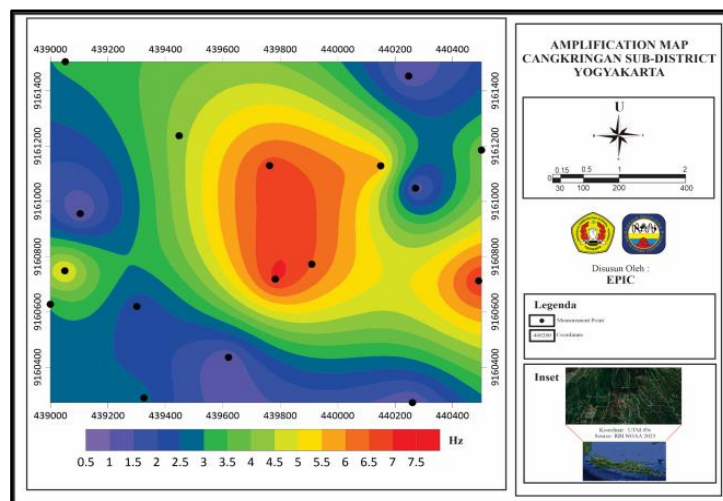


**Figure 5.** Amplification Map of Cangkringan Sub-District  
Source: Data Processing, 2024

In conclusion, the amplification results offer a detailed understanding of seismic risks in the Cangkringan District. The findings highlight the importance of targeted disaster preparedness and risk reduction efforts in high-risk zones while also providing a basis for urban planning and infrastructure development in safer areas. These results contribute to building a more resilient community capable of withstanding seismic hazards.

### Dominant Frequency

Dominant frequency is a critical parameter in understanding soil dynamics, as it reflects the natural frequency of subsurface layers and their response to seismic waves. This frequency is primarily influenced by subsurface velocity and the thickness of sediment layers. Areas with thicker sediment deposits generally exhibit lower dominant frequencies, while regions with thinner or denser layers of hard rock tend to show

higher frequencies (Housner, 1983). The dominant frequency values derived from this study provide important insights into the geological conditions of the Cangkringan District.

The dominant frequency values in the study area ranged from 1.5 Hz to 14 Hz. These values were classified into four types based on Kanai's classification, as shown in Table 2. Type I, with a dominant frequency of 6.67–20 Hz, is associated with hard gravelly sandstone and very thin surface sediment layers. Type II, with a frequency range of 4–10 Hz, corresponds to alluvial rock layers with a moderate sediment thickness of approximately 5–10 meters. Type III, characterized by frequencies of 2.5–4 Hz, represents areas with thicker sediment layers, typically 10–30 meters, composed of alluvial deposits. Type IV, with frequencies below 2.5 Hz, is indicative of very thick sediment layers formed from deltaic sedimentation, mud, or soft soil, with thicknesses exceeding 30 meters.

**Table 2.** Classification of Dominant Frequency

Soil Classification	Dominant Frequency (Hz)	Kanai Classification	Description
<b>Type I</b>	6.67-20	Tertiary or older rocks, consisting of hard gravelly sandstone	The thickness of the surface sediment layer is thin. Dominated by hard rock.
<b>Type II</b>	10-4	Alluvial rock with a thickness of 5m consists of sand, gravel, hard sandy clay, clay, etc.	The thickness of the surface sediment layer is 5-10m
<b>Type III</b>	2.5-4	Alluvial rocks which are almost the same as type II, are differentiated into unknown formations	The surface sediment layer falls within the thick category, with a thickness ranging between 10 and 30 meters.
<b>Type IV</b>	<2.5	Alluvial rock formed form deltaic sedimentation, topsoil, mud, humus, soft soil, deltaic or silt deposit, soft soil with depth of 30m.	The surface sediment layer exhibits substantial thickness.

Source: Housner (1983)

Figure 6 illustrates the dominant frequency map for the Cangkringan Sub-District. This map highlights the spatial distribution of frequency values and provides a detailed overview of subsurface conditions. Areas classified as Type I, represented in red, are characterized by thin sediment layers and hard rock formations. These regions are less susceptible to seismic amplification due to their dense subsurface composition. Areas classified as Type II, shown in yellow and green, have moderate sediment thickness and are moderately susceptible to seismic amplification. In contrast, Type III areas, represented in blue, and Type IV areas, depicted in purple, are associated with thicker sediment layers. These regions exhibit lower dominant frequencies, making them more vulnerable to seismic amplification and potential liquefaction during earthquakes.

The dominant frequency results provide valuable information for seismic hazard assessment and disaster preparedness planning. Low-frequency areas, particularly those classified as Type IV, are of significant concern due to their thick, soft sediment layers, which can amplify seismic waves. These zones require careful consideration in land-use planning, as they pose a higher risk for structural damage during seismic events. Conversely, high-frequency zones, such as those classified as Type I, are relatively stable and suitable for the placement of critical infrastructure and disaster response facilities.

Integrating the dominant frequency data with other seismic parameters, such as amplification,  $V_s30$ , and seismic susceptibility enhances the understanding of the study area's seismic vulnerability. This integration supports the development of a comprehensive mitigation framework, ensuring that disaster response strategies are both effective and scientifically grounded. For instance, evacuation routes and disaster posts should be located in high-frequency zones to minimize exposure to seismic amplification and ensure the safety of residents and tourists.

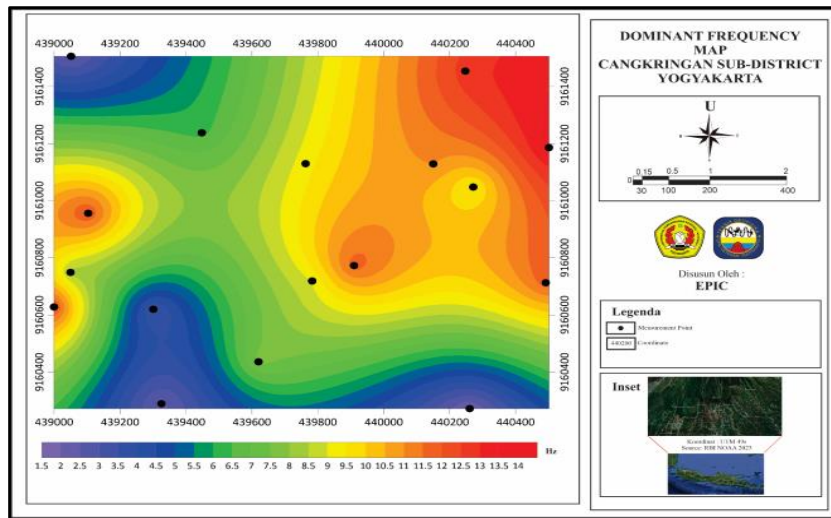


**Figure 6.** Dominant Frequency Map of Cangkringan Sub-District  
Source: Data Processing, 2024

In conclusion, the dominant frequency analysis provides a nuanced understanding of the subsurface dynamics in the Cangkringan District. The results emphasize the importance of prioritizing low-frequency zones for targeted risk reduction measures while leveraging high-frequency zones for safer infrastructure and disaster preparedness efforts. These findings contribute to building a resilient geotourism framework and enhancing the overall safety of the region.

### Seismic Vulnerability (Kg)

Seismic vulnerability, often expressed as the Seismic Vulnerability Index (Kg), is a measure of how susceptible a specific area is to damage from seismic activity. This parameter is determined by evaluating the dominant frequency and amplification values of the subsurface. Areas with high seismic vulnerability are typically characterized by soft soil layers, low-density materials, and high amplification, which amplify ground shaking during an earthquake. The Seismic Vulnerability Index provides essential information for identifying zones prone to seismic hazards and is critical for disaster preparedness and mitigation efforts.

In this study, the seismic vulnerability values in the Cangkringan District ranged from 0 s<sup>2</sup>/cm to 5.6 s<sup>2</sup>/cm. Based on Prabowo et al. (2018) classification, these values were categorized into three groups: low vulnerability (<10 s<sup>2</sup>/cm), moderate vulnerability (10 < Kg < 20 s<sup>2</sup>/cm), and high vulnerability (>20 s<sup>2</sup>/cm). The results show that most of the study area falls within the low and moderate vulnerability zones, with only a few areas exhibiting high seismic vulnerability.

**Table 3.** Classification of Seismic Vulnerability

Classification	Seismic Vulnerability Value
< 10	Low
10 < Kg < 20	Currently
> 20	Danger

Source: Prabowo (2018)

The seismic vulnerability map, as presented in Figure 7, provides a detailed spatial representation of the Kg values across the study area. Areas with low seismic vulnerability, shown in blue to purple, have values below 1.6 s<sup>2</sup>/cm. These zones are dominated by dense rock formations with minimal density contrasts between layers, making them less susceptible to seismic amplification. Moderate seismic vulnerability zones, represented in green to yellow, have values ranging from 2 s<sup>2</sup>/cm to 3.6 s<sup>2</sup>/cm. These areas are characterized by moderately dense soil and some variation in subsurface properties. High seismic vulnerability zones, depicted in orange to red, have values between 4 s<sup>2</sup>/cm and 5.6 s<sup>2</sup>/cm. These regions

are associated with soft soil layers, thick sediments, and significant density contrasts, making them highly susceptible to ground shaking and structural damage during earthquakes.

The seismic vulnerability analysis highlights critical areas that require targeted disaster risk reduction measures. High-vulnerability zones, particularly those with red and orange values on the map, are of significant concern as they are more likely to experience severe damage during seismic events. These areas should be avoided for critical infrastructure development and are not suitable for the placement of disaster response facilities. Conversely, low-vulnerability zones, shown in blue and purple, offer greater stability and are ideal locations for evacuation routes, disaster mitigation posts, and safe shelters for residents and tourists.

The integration of seismic vulnerability data with other seismic parameters, such as amplification, dominant frequency, and  $V_{s30}$ , enhances the accuracy of the risk assessment. This comprehensive approach provides a more detailed understanding of the geological hazards in the study area, enabling the development of effective mitigation strategies. For example, the combination of low  $K_g$  values, high  $V_{s30}$  values, and low amplification ensures the identification of optimal sites for disaster posts and evacuation pathways.

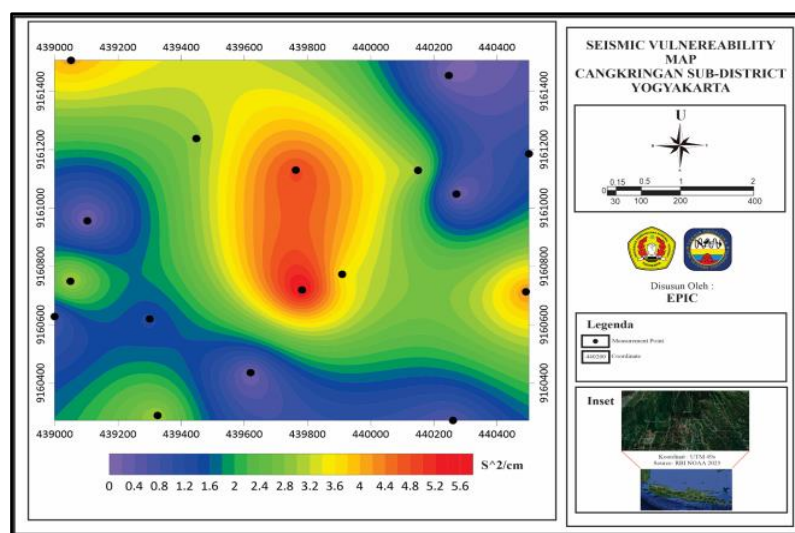


**Figure 7.** Seismic Vulnerability Map of Cangkringan Sub-District  
Source: Data Processing, 2024

In conclusion, the seismic vulnerability analysis provides a clear understanding of the Cangkringan District's susceptibility to seismic hazards. The results emphasize the importance of prioritizing high-vulnerability zones for disaster risk reduction measures, such as retrofitting existing structures and restricting new developments. Simultaneously, low-vulnerability zones can be leveraged for safer infrastructure and disaster preparedness initiatives. This study's findings contribute to improving community resilience and ensuring the safety of both residents and tourists in this high-risk region.

### Peak Ground Acceleration (PGA)

Peak Ground Acceleration (PGA) is a vital parameter for assessing the intensity of ground shaking during an earthquake. It represents the maximum acceleration experienced by the ground, providing critical information for seismic hazard assessments and structural resilience planning (Elizabeth Philip & Helen Santhi, 2020). In this study, PGA values in the Cangkringan District ranged from 450 gal to 1300 gal, reflecting the varying levels of seismic risk across the area. These values were classified into distinct intensity levels, as shown in Table 4, based on the Modified Mercalli Intensity (MMI) scale and their corresponding effects on buildings, infrastructure, and the environment.

The low-intensity PGA range (1–2 gal) corresponds to MMI Level I, where seismic activity is barely felt, with no structural damage expected. This is followed by MMI Level II (2–5 gal), characterized by noticeable shaking and minor damage to poorly constructed buildings. The intensity gradually increases to MMI Level III (5–10 gal), where seismic waves are felt inside houses, resembling the effect of a passing truck. Higher PGA values within the 10–25-gal range (MMI Level IV) result in strong vibrations that feel

like a heavy object hitting a wall, while MMI Level V shaking is severe enough to disturb outdoor activities, awaken sleeping individuals, and cause minor spills or breakages.

Significant structural damage begins to occur at PGA values exceeding 50 gal (MMI Level VII), where ground motion is intense enough to break chimneys and disrupt car driving. As the PGA reaches the 100–250-gal range (MMI Level VIII), there is visible damage to strong buildings, with collapsed parts posing serious risks. The 250–500-gal range (MMI Level IX) is associated with widespread panic, the destruction of weak buildings, and severe foundational damage to stronger structures. At the highest level of 500–1000 gal (MMI Level X), nearly all structures, including walls, frames, and foundations, sustain severe damage. Dams, embankments, and bridges are compromised, and large landslides occur, representing catastrophic consequences for the region.

The spatial distribution of PGA values is depicted in Figure 8: Peak Ground Acceleration Map of Cangkringan Sub-District. Areas with low PGA values (450–700 gal) are marked in blue and purple, typically associated with dense rock formations that resist seismic wave amplification. These zones are less susceptible to significant damage, making them ideal locations for critical infrastructure and disaster response facilities. Areas with medium PGA values (750–1000 gal) are shown in green to yellow. These regions exhibit moderate seismic risk and may experience minor to moderate structural damage during an earthquake. Conversely, areas with high PGA values (1050–1300 gal) are represented in orange and red. These zones are associated with soft soils and thick sediment layers, which amplify seismic waves, increasing the likelihood of severe ground shaking and structural collapse.

**Table 4.** Intensity Based on Impact and Maximum Ground Acceleration

PGA (gal)	Intensity	Effect
1-2	I	Barely felt; unlikely to cause damage.
2-5	II	Noticeable shaking; minor damage to poorly constructed buildings.
5-10	III	Felt inside the house, as if a truck was passing by but many did not expect an earthquake.
	IV	Felt inside the house like a truck is passing or feels like a heavy object has hit the wall of the house.
	V	Can be felt outside the house, sleeping person wakes up, fluids appear to move and spill slightly.
10-25	VI	Felt by everyone. Many people run outside in shock, people walking are disturbed, windows crack, pottery, and glassware shatter.
	VII	It can be felt by the driver who is driving; difficult for pedestrians to walk properly, weak chimneys break.
50-100	VIII	Car driving is disturbed, and there is damage to strong buildings due to parts collapsing.
100-250	IX	The public panics: weak buildings are destroyed, and strong buildings suffer heavy damage, including foundations.
250-500	X	The public panics: weak buildings are destroyed, and strong buildings suffer heavy damage, including foundations.

Source: [Margottini et al. \(1992\)](#)

The results emphasize the importance of integrating PGA data into disaster preparedness and urban planning. High PGA zones, which are most vulnerable to seismic damage, require immediate attention for retrofitting and risk reduction measures. Conversely, low PGA zones can be leveraged for evacuation routes, disaster mitigation posts, and safe shelters for residents and tourists. By combining PGA values with other seismic parameters, such as amplification and seismic vulnerability ( $K_g$ ), a comprehensive mitigation framework was developed, ensuring effective disaster response and infrastructure planning.

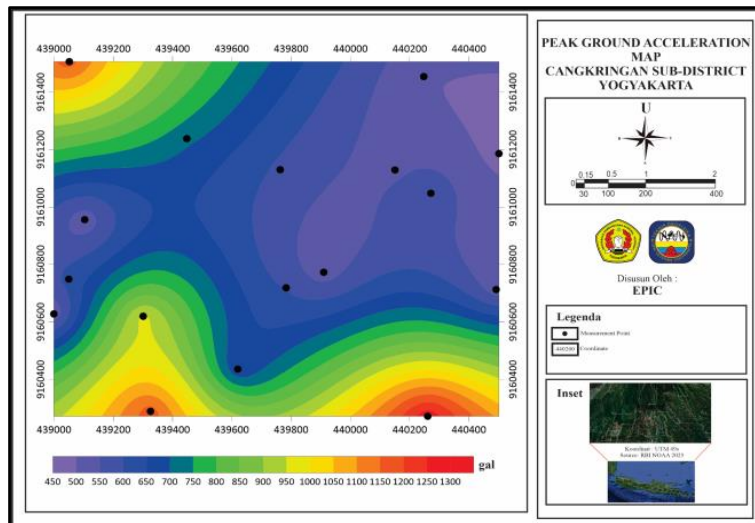


**Figure 8.** Peak Ground Acceleration Map of Cangkringan Sub-District  
Source: Data Processing, 2024

In conclusion, the PGA analysis provides a clear understanding of the seismic risks in the Cangkringan District. The results, supported by Table 4 and Figure 8, highlight the need for targeted interventions in high-risk zones while prioritizing low-risk areas for safe infrastructure development. These findings contribute to reducing seismic hazards and improving the resilience of the community and geotourism activities in the region.

### Vs30 Map

The Vs30 parameter represents the average shear wave velocity of the top 30 meters of subsurface soil and rock layers. It is a widely used metric in seismic studies, as it reflects the stiffness and density of the upper subsurface layers, which significantly influence ground shaking during an earthquake. Higher Vs30 values correspond to denser and stiffer materials, providing greater resistance to seismic wave propagation, while lower Vs30 values indicate softer and more flexible soils that amplify seismic waves.

In this study, the Vs30 values in the Cangkringan District ranged from 300 m/s to 550 m/s, providing a detailed understanding of the area's subsurface characteristics. These values were classified according to the National Earthquake Hazards Reduction Program (NEHRP) standards (FEMA, 1997), as shown in Table 5. Zones with Vs30 values > 1500 m/s (Type A) represent hard rock formations, while Vs30 values between 760–1500 m/s (Type B) correspond to rock. Vs30 values between 300–760 m/s (Type C) indicate very dense soils or soft rock, and Vs30 values between 180–360 m/s (Type D) represent stiff soils. Vs30 values < 180 m/s (Type E) are associated with soft soils, which are highly vulnerable to seismic amplification.

**Table 5.** Classification of Rock Types Based on Value Vs30 Standard NHERP

Type Rock	Profile Type Rock	Vs30 (m/s)
A	Hard Rock (SA)	>1500 m/s
B	Rock (Rock Currently)	760 - 1500 m/s
C	Very Dense Soil and Soft Rock (Land Hard and Rock soft)	300 - 760 m/s
D	Stiff Soil (Land Currently)	180-360 m/s
E	Soft Soil (Land Soft)	<180 m/s

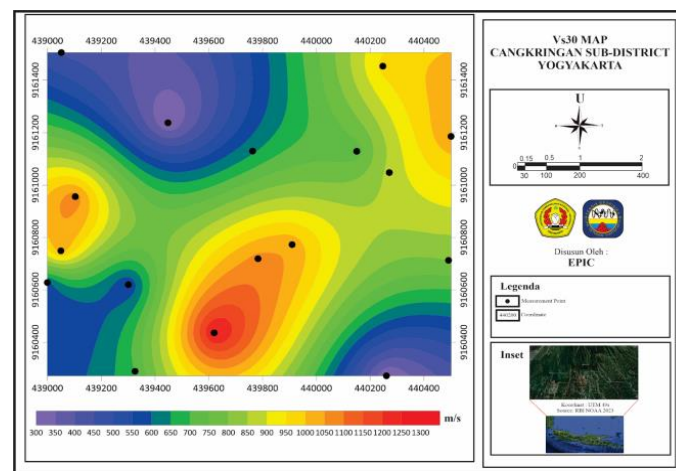
Source: Xie et al. (2023)

Figure 9 illustrates the spatial distribution of shear wave velocities across the region. Areas with higher Vs30 values (500–550 m/s), shown in green to blue, are located in regions dominated by hard rock and very dense soil. These zones exhibit low seismic amplification potential and are considered safer for infrastructure development and disaster mitigation efforts. In contrast, areas with lower Vs30 values (300–

400 m/s), marked in yellow to orange, are associated with softer soils and thicker sediment layers. These zones are prone to significant seismic wave amplification, posing a higher risk of structural damage during earthquakes.

The Vs30 map highlights the critical role of subsurface stiffness in determining seismic risk. Regions with low Vs30 values are of particular concern, as they are more likely to experience intense ground shaking and liquefaction during seismic events. These areas should be prioritized for seismic risk reduction measures, including retrofitting existing structures and implementing strict building codes for new developments. Conversely, high Vs30 zones provide a stable foundation for evacuation routes, disaster response facilities, and other critical infrastructure.

By integrating the Vs30 data with other seismic parameters, such as Peak Ground Acceleration (PGA), amplification, and seismic vulnerability (Kg), a comprehensive risk assessment was conducted for the Cangkringan District. This integration enabled the identification of safe zones for disaster posts and evacuation pathways while highlighting high-risk areas requiring targeted interventions.



**Figure 9.** Vs30 Map of Cangkringan Sub-District  
Source: Data Processing, 2024

In conclusion, the Vs30 analysis provides valuable insights into the subsurface conditions of the Cangkringan District. The results, supported by Table 5 and Figure 9, emphasize the importance of using Vs30 data to guide disaster preparedness and urban planning. The findings contribute to building a more resilient community capable of withstanding seismic hazards while supporting sustainable geotourism development in the region.

### Ground Shear Strain (GSS)

Ground Shear Strain (GSS) is a critical parameter for assessing the deformation potential of soils under seismic stress. It reflects the strain experienced by the ground during an earthquake, calculated from the combination of seismic susceptibility (Kg) and Peak Ground Acceleration (PGA). High GSS values are indicative of areas with significant deformation potential, such as liquefaction, ground settlement, or landslides, posing severe risks to infrastructure and human safety. In contrast, low GSS values suggest stable zones with minimal seismic deformation risk. This analysis is essential for seismic hazard mitigation and disaster preparedness.

**Table 6.** Classification of Ground Shear Strain ( $\gamma$ ) Values and Soil Dynamic Properties

The Value of ground shear strain ( $\gamma$ )	$10^{-6}$ $10^{-5}$	$10^{-4}$ $10^{-3}$	$10^{-2}$ $10^{-1}$
Phenomenon	Seismic Waves, Vibrations	Crack, Soil Settlement (Differential Settlement)	Landslide, Soil Compaction, Liquefaction

Source: Hou et al. (2023)

In the Cangkringan District, GSS values ranged from  $10^{-4}$  to  $8.5 \times 10^{-4}$ , as shown in Figure 10: Ground Shear Strain Map of Cangkringan Sub-District. Low GSS zones, depicted in purple and blue, correspond to dense rock formations and compact soils, which exhibit high resistance to seismic deformation. These areas are considered safe for critical infrastructure development, such as evacuation routes and disaster response facilities. Conversely, high GSS zones, marked in yellow to red, indicate regions with soft soils and thick sedimentary layers, which are more prone to seismic amplification and deformation. These areas require urgent interventions, such as retrofitting existing structures and implementing stricter building codes.

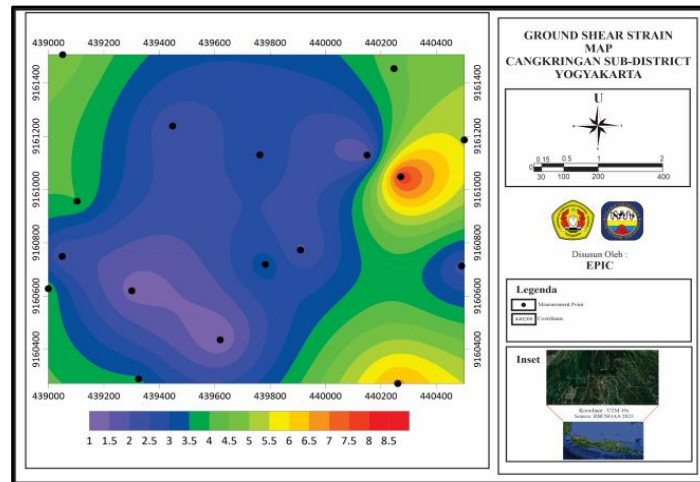


**Figure 10.** Ground Shear Strain Map of Cangkringan Sub-District  
Source: Data Processing, 2024

The spatial analysis is further enhanced by Figure 11: Complete Bouguer Anomaly Map of Cangkringan Sub-District, which highlights subsurface density variations. Low-density zones, represented in darker shades, align with areas of high GSS values, typically associated with soft sedimentary layers or alluvial deposits. High-density zones, shown in lighter colors, correspond to igneous or metamorphic rock formations, which exhibit low GSS values. This correlation provides valuable insights into the geological factors contributing to seismic risk in the area.

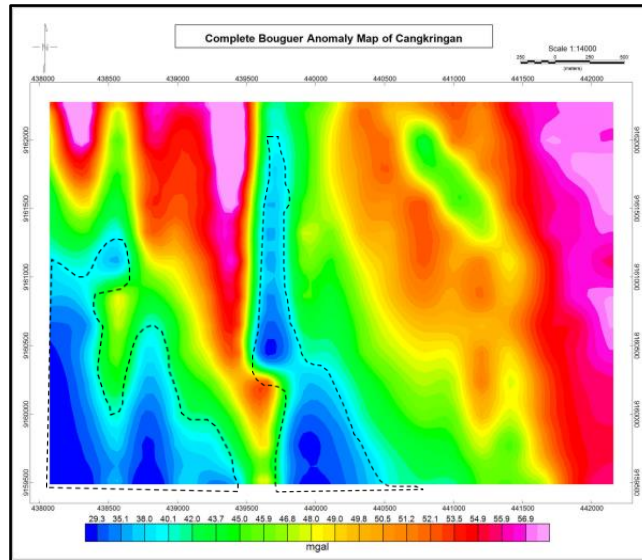


**Figure 11.** Complete Bouguer Anomaly Map of Cangkringan Sub-District  
Source: Data Processing, 2024

Figure 12: Mitigation Map Based on GSS, Vs30, and Seismic Vulnerability (Kg) integrates multiple seismic parameters, offering a comprehensive risk assessment of the Cangkringan District. This map identifies safe zones for disaster mitigation posts and evacuation routes by prioritizing areas with low GSS values, high Vs30 values, and low seismic vulnerability. These zones represent stable regions with minimal seismic risk, ensuring the safety of both residents and tourists. Conversely, high-risk zones with high GSS values and low Vs30 values are marked as unsuitable for critical infrastructure, highlighting the need for targeted risk reduction measures.

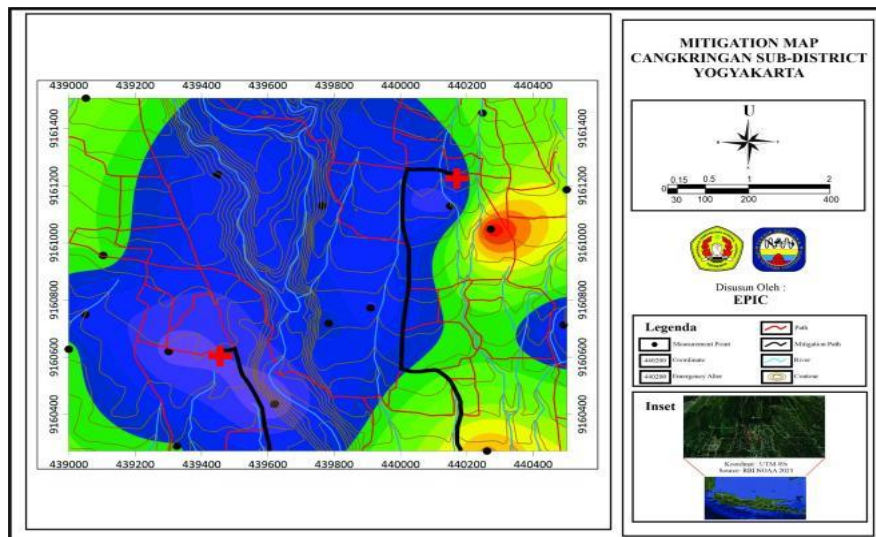


**Figure 12.** Mitigation Map Based on GSS, Vs30, and Seismic Vulnerability (Kg)  
Source: Data Processing, 2024

In conclusion, the GSS analysis, supported by Figures 11 and 12, provides a detailed understanding of seismic risks in the Cangkringan District. High GSS zones require immediate attention for disaster risk reduction, while low GSS zones offer safe foundations for critical infrastructure development. By integrating GSS data with Vs30 and Bouguer anomaly findings, this study ensures a holistic approach to seismic hazard mitigation, contributing to enhanced resilience and sustainable planning in the region.

## Implications

This study provides critical insights into the seismic hazards and subsurface characteristics of the Cangkringan District, offering significant implications for disaster management, infrastructure planning, and sustainable development in high-risk areas. By integrating microseismic and gravity methods, the research establishes a robust framework for assessing seismic vulnerabilities, which can be applied to similar disaster-prone regions worldwide. Recent studies have emphasized the importance of combining multiple geophysical techniques to improve hazard assessments and risk mitigation strategies in areas with complex geological conditions (Chopra et al., 2023; Nakamura, 1999). The integration of these methods ensures a more comprehensive understanding of subsurface dynamics, enhancing the accuracy of seismic risk mapping.

The findings highlight the importance of disaster risk reduction through the identification of high-risk zones with amplified seismic vulnerability, high Peak Ground Acceleration (PGA), and low  $V_{s30}$  values. These areas require immediate attention, including retrofitting existing infrastructure, enforcing strict building regulations, and restricting developments in zones prone to liquefaction and ground deformation. Studies by Bai et al. (2022) and Namjesnik et al. (2021) have demonstrated the effectiveness of retrofitting and targeted land-use policies in reducing seismic damage and improving resilience in similar high-risk regions. The identification of low-risk zones with stable ground conditions also provides actionable guidance for the strategic placement of disaster mitigation posts and evacuation routes, ensuring effective disaster preparedness and response. This aligns with findings by Hsu & Sharma (2023), which highlighted the role of strategically located safe zones in minimizing casualties during seismic events.

The study offers valuable implications for urban planning and infrastructure development. By identifying stable areas with low seismic amplification and dense subsurface formations, the findings provide a foundation for resilient urban development. These insights can guide policymakers and urban planners in optimizing land use and prioritizing safety in constructing residential areas, critical infrastructure, and tourism facilities. Recent research by Wulung & Abdullah (2021) emphasized the importance of integrating geophysical data into urban planning to enhance structural resilience and reduce long-term economic losses. Such planning not only mitigates potential earthquake damage but also enhances the overall safety and sustainability of the region.

Additionally, the integration of geophysical data into disaster preparedness strategies strengthens community resilience by equipping residents and stakeholders with the tools and knowledge to mitigate seismic risks. This research underscores the value of community-centered approaches, as highlighted by Alhaffar et al. (2023), which advocate for combining technical assessments with community engagement to foster proactive measures and improve disaster awareness. By integrating safety considerations into planning, the study contributes to building a resilient society capable of effectively responding to seismic events and recovering quickly from their impacts.

The implications of this research extend to the development of geotourism in the Merapi slope area. By addressing safety concerns and integrating disaster management into tourism planning, the findings enhance tourists' trust and confidence in visiting the region. Recent studies, such as those by Rindrasi et al. (2024), have shown that disaster risk management in tourism areas significantly influences visitor satisfaction and long-term sustainability. This dual focus on safety and tourism development ensures that the area remains an attractive destination while minimizing risks to visitors. The integration of disaster risk reduction measures into geotourism not only protects lives but also supports the long-term economic sustainability of the region.

Finally, this study makes a significant contribution to the scientific understanding of seismic hazards by demonstrating the utility of combining microseismic and gravity methods for comprehensive seismic risk assessments. Policymakers can leverage these findings to design data-driven strategies that balance safety, economic growth, and environmental sustainability. By aligning with global frameworks such as the Sendai Framework for Disaster Risk Reduction, this research reinforces the necessity of proactive measures to enhance community resilience and reduce the impacts of seismic hazards. The findings also resonate with global best practices for disaster risk management, as documented in the United Nations' latest disaster preparedness reports (Bailey, 2022).

## CONCLUSION

This study provides a comprehensive assessment of seismic hazards in the Cangkringan District, Sleman Regency, using integrated micro seismic and gravity methods. The analysis highlights the varying seismic risks across the region by evaluating key parameters such as amplification, dominant frequency, Peak Ground Acceleration (PGA),  $V_{s30}$ , and Ground Shear Strain (GSS). The findings reveal significant spatial variations in subsurface characteristics, which directly influence seismic vulnerability and potential ground deformation.

The results underscore the critical need for targeted disaster risk reduction measures in high-risk zones characterized by high amplification, low  $V_{s30}$  values, and elevated GSS levels. These areas are particularly vulnerable to seismic amplification and liquefaction, requiring immediate interventions, including retrofitting of existing structures, enforcement of strict building codes, and strategic land-use planning. Conversely, low-risk zones, identified by stable ground conditions, provide suitable locations for disaster mitigation posts, evacuation routes, and critical infrastructure development.

The study also contributes to urban planning by offering actionable insights into optimizing land use in the region. By identifying stable areas with minimal seismic risks, the findings support the development of resilient residential zones, tourism facilities, and infrastructure. Moreover, the integration of disaster risk reduction measures into geotourism planning enhances the safety and sustainability of tourism activities in the Merapi slope area, ensuring the long-term viability of this economically vital sector.

From a scientific perspective, this research demonstrates the effectiveness of integrating microseismic and gravity methods for comprehensive seismic hazard assessments. The methodology provides a replicable framework for similar studies in other disaster-prone regions, emphasizing the importance of combining geophysical data for a holistic understanding of subsurface dynamics and seismic risks.

In conclusion, the study highlights the importance of proactive disaster preparedness and sustainable urban planning in mitigating seismic risks and enhancing community resilience. By addressing the unique challenges posed by the region's geological and seismic conditions, the findings provide a valuable foundation for safeguarding lives, infrastructure, and economic activities in the Cangkringan District. These contributions align with global disaster risk reduction goals, ensuring that the region is better prepared to withstand and recover from seismic events.

## Disclosure Statement

The authors declare no potential conflicts of interest with respect to the research, authorship, and publication of this study.

## REFERENCES

- Alhaffar, M. B. A., Jouiry, E., & Eriksson, A. (2023). Community engagement and crowdsourcing for effective disaster response and rescue operations during the earthquake in Syria. *International Journal of Disaster Risk Reduction*, 98, 104096. <https://doi.org/10.1016/j.ijdr.2023.104096>
- Alonso-Pandavenes, O., Bernal, D., Torrijo, F. J., & Garzón-Roca, J. (2023). A Comparative Analysis for Defining the Sliding Surface and Internal Structure in an Active Landslide Using the HVSR Passive Geophysical Technique in Pujilí (Cotopaxi), Ecuador. *Land*, 12(5), 961. <https://doi.org/10.3390/land12050961>
- Bai, J., Dou, L., Cai, W., Gong, S., Shen, W., Tian, X., & Ma, H. (2022). An Integration Method of Bursting Strain Energy and Seismic Velocity Tomography for Coal Burst Hazard Assessment. *Lithosphere*, 2022(Special 11), 2070540. <https://doi.org/10.2113/2022/2070540>
- Bailey, E. (2022). Disaster Risk Reduction and Management: Recalling the Need for Paradigm Shift in Definition. *Journal of Geoscience and Environment Protection*, 10(06), 86–105. <https://doi.org/10.4236/gep.2022.106006>
- Beroya, M. A. A., Aydin, A., Tiglao, R., & Lasala, M. (2009). Use of microtremor in liquefaction hazard mapping. *Engineering Geology*, 107(3–4), 140–153. <https://doi.org/10.1016/j.enggeo.2009.05.009>
- Brigola. (2025). *Fourier Analysis and Distributions* (1st ed.). Springer. <https://link.springer.com/book/9783031813108>

- Chopra, S., Choudhury, P., Nikam, R., Chaudhary, P., Limbachiya, H., & Joshi, V. (2023). Use of Geophysical Techniques in Seismic Hazard Assessment and Microzonation. In Sandeep, P. Kumar, H. Mittal, & R. Kumar (Eds.), *Geohazards* (Vol. 53, pp. 73–87). Springer Nature Singapore. [https://doi.org/10.1007/978-981-99-3955-8\\_5](https://doi.org/10.1007/978-981-99-3955-8_5)
- Diaz-Segura, E. G., Vielma, J. C., & Oviedo-Veas, J. E. (2024). Microzonation Approach for Analyzing Regional Seismic Response: A Case Study of the Dune Deposit in Concón, Chile. *Applied Sciences*, *14*(18), 8458. <https://doi.org/10.3390/app14188458>
- Dowling, R. K. (2011). Geotourism's Global Growth. *Geoheritage*, *3*(1), 1–13. <https://doi.org/10.1007/s12371-010-0024-7>
- Elizabeth Philip, S., & Helen Santhi, M. (2020). Peak Ground Acceleration Analysis using Past Earthquake Data. *Journal of Physics: Conference Series*, *1716*(1), 012013. <https://doi.org/10.1088/1742-6596/1716/1/012013>
- Hou, T., Cui, Y., Pan, X., Luo, Y., & Liu, Q. (2023). Characteristics of dynamic shear modulus and damping ratio and the structural formula of EPS particles lightweight soil. *Soil Dynamics and Earthquake Engineering*, *166*, 107768. <https://doi.org/10.1016/j.soildyn.2023.107768>
- Hou, Y., Jiao, R., & Yu, H. (2021). MEMS based geophones and seismometers. *Sensors and Actuators A: Physical*, *318*, 112498. <https://doi.org/10.1016/j.sna.2020.112498>
- Housner, G. (1983). Engineering seismology, by Kiyoshi Kanai, University of Tokyo Press, 1983. No. of pages: 251. *Earthquake Engineering & Structural Dynamics*, *11*(5), 727–728. <https://doi.org/10.1002/eqe.4290110511>
- Hsu, J. L., & Sharma, P. (2023). Disaster and risk management in outdoor recreation and tourism in the context of climate change. *International Journal of Climate Change Strategies and Management*, *15*(5), 712–728. <https://doi.org/10.1108/IJCCSM-10-2021-0118>
- Liu, P.-H., Wu, J.-H., Lee, D.-H., & Lin, Y.-H. (2023). Detecting landslide vulnerability using anisotropic microtremors and vulnerability index. *Engineering Geology*, *323*, 107240. <https://doi.org/10.1016/j.enggeo.2023.107240>
- Margottini, C., Molin, D., & Serva, L. (1992). Intensity versus ground motion: A new approach using Italian data. *Engineering Geology*, *33*(1), 45–58. [https://doi.org/10.1016/0013-7952\(92\)90034-V](https://doi.org/10.1016/0013-7952(92)90034-V)
- Mishra, D. C. (2024). *Gravity and Magnetic Methods for Geological Studies: Principles, Integrated Exploration and Plate Tectonics* (1st edition). CRC Press.
- Nakamura, Y. (1999). *Clear Identification of Fundamental Idea of Nakamura ' S Technique And Its Applications*. <https://api.semanticscholar.org/CorpusID:56568879>
- Namjesnik, D., Kinscher, J., Gunzburger, Y., Poiata, N., Dominique, P., Bernard, P., & Contrucci, I. (2021). Automatic Detection and Location of Microseismic Events from Sparse Network and Its Application to Post-mining Monitoring. *Pure and Applied Geophysics*, *178*(8), 2969–2997. <https://doi.org/10.1007/s00024-021-02773-4>
- Neukirch, M., García-Jerez, A., Villaseñor, A., Luzón, F., Ruiz, M., & Molina, L. (2021). Horizontal-to-Vertical Spectral Ratio of Ambient Vibration Obtained with Hilbert–Huang Transform. *Sensors*, *21*(9), 3292. <https://doi.org/10.3390/s21093292>
- Pant, Y. R. (2023). Participation in Disaster Risk Reduction (DRR) Education: Analysing the Practices, Issues and Challenges. *Open Journal of Earthquake Research*, *12*(04), 198–222. <https://doi.org/10.4236/ojer.2023.124008>
- Prabowo, U. N., Amalia, A. F., & Wiranata, F. E. (2018). Local site effect of soil slope based on microtremor measurement in Samigaluh, Kulon Progo Yogyakarta. *Journal of Physics: Conference Series*, *997*, 012007. <https://doi.org/10.1088/1742-6596/997/1/012007>
- Putriani, E., Wu, Y.-M., Chen, C.-W., Ismulhadi, A., & Fadli, D. I. (2023). Development of landslide susceptibility mapping with a multi-variance statistical method approach in Kepahiang Indonesia. *Terrestrial, Atmospheric and Oceanic Sciences*, *34*(1), 18. <https://doi.org/10.1007/s44195-023-00050-6>
- Rindrasi, E., Ratminto, Effendi, K. C., & Silviani, D. (2024). Expert perspectives on disaster risk reduction strategies in the tourist area of Borobudur-Yogyakarta-Prambanan in Indonesia. *Progress in Disaster Science*, *24*, 100379. <https://doi.org/10.1016/j.pdisas.2024.100379>
- Sollberger, D., Igel, H., Schmelzbach, C., Edme, P., Van Manen, D.-J., Bernauer, F., Yuan, S., Wassermann, J., Schreiber, U., & Robertsson, J. O. A. (2020). Seismological Processing of Six Degree-of-Freedom Ground-Motion Data. *Sensors*, *20*(23), 6904. <https://doi.org/10.3390/s20236904>

- Surono, Jousset, P., Pallister, J., Boichu, M., Buongiorno, M. F., Budisantoso, A., Costa, F., Andreastuti, S., Prata, F., Schneider, D., Clarisse, L., Humaida, H., Sumarti, S., Bignami, C., Griswold, J., Carn, S., Oppenheimer, C., & Lavigne, F. (2012). The 2010 explosive eruption of Java's Merapi volcano— A '100-year' event. *Journal of Volcanology and Geothermal Research*, 241–242, 121–135. <https://doi.org/10.1016/j.jvolgeores.2012.06.018>
- Thouret, J.-C., Lavigne, F., Kelfoun, K., & Bronto, S. (2000). Toward a revised hazard assessment at Merapi volcano, Central Java. *Journal of Volcanology and Geothermal Research*, 100(1–4), 479–502. [https://doi.org/10.1016/S0377-0273\(00\)00152-9](https://doi.org/10.1016/S0377-0273(00)00152-9)
- Wulung, S. R. P., & Abdullah, C. U. (2021). Disaster Literacy on Geotourism Routes. *Journal of Engineering Science and Technology*, 5, 60–69.
- Xie, J., Li, K., Li, X., An, Z., & Wang, P. (2023). VS30-based relationship for Chinese site classification. *Engineering Geology*, 324, 107253. <https://doi.org/10.1016/j.enggeo.2023.107253>
- Yudiantoro, D., Koly, J., & Haty, P. (2023). Analisis Deformasi Gunung Api Merapi, Melalui Penerapan Metode Kombinasi Block Movement dan Deformasi Elastis, Pada Periode Tahun 1995-1997 Berdasarkan Data Gps (Global Positioning System). *Jurnal Ilmiah Geologi PANGEA*.
- Yulianto, T., & Yuliyanto, G. (2023). Microtremor data and HVSR method in the kaligarang fault zone Semarang, Indonesia. *Data in Brief*, 49, 109428. <https://doi.org/10.1016/j.dib.2023.109428>
- Zewde, S. M. (2023). Information Management in Disaster and Humanitarian Response: A Case in United Nations Office for the Coordination of Humanitarian Affairs. *Intelligent Information Management*, 15(02), 47–65. <https://doi.org/10.4236/iim.2023.152004>